Check for updates

AGU ADVANCING EARTH AND SPACE SCIENCES

Geophysical Research Letters

RESEARCH LETTER
10.1029/2023GL106613

Climatic Drivers of Ice Slabs and Firn Aquifers in Greenland

M. Brils[1], P. Kuipers Munneke[1], N. Jullien[2], A. J. Tedstone[2], H. Machguth[2], W. J. van de Berg[1], and M. R. van den Broeke[1]

[1]Institute for Marine and Atmospheric Research, Utrecht University, Utrecht, The Netherlands, [2]Department of Geosciences, University of Fribourg, Fribourg, Switzerland

Key Points:

- Accumulation, melt and rain are good predictors of ice slab and firn aquifer locations
- The expansion of modeled ice slabs and aquifers on the Greenland ice sheet started in the early 2000s
- We show that, in between the ablation zone and the accumulation zone, there are always ice slabs and/or aquifers present

Supporting Information:

Supporting Information may be found in the online version of this article.

Correspondence to:

M. Brils,
m.brils@uu.nl

Citation:

Brils, M., Munneke, P. K., Jullien, N., Tedstone, A. J., Machguth, H., van de Berg, W. J., & van den Broeke, M. R. (2024). Climatic drivers of ice slabs and firn aquifers in Greenland. *Geophysical Research Letters*, *51*, e2023GL106613. https://doi.org/10.1029/2023GL106613

Received 4 OCT 2023
Accepted 22 JAN 2024

© 2024. The Authors.
This is an open access article under the terms of the Creative Commons Attribution-NonCommercial-NoDerivs License, which permits use and distribution in any medium, provided the original work is properly cited, the use is non-commercial and no modifications or adaptations are made.

Abstract Recent observations revealed the existence of ice slabs and aquifers on the Greenland ice sheet (GrIS). Both affect the ice sheet's hydrology: ice slabs facilitate runoff and aquifers modulate drainage to the bed. However, their climatic drivers and history remain unclear, as most observations cover only two decades. Here, we present a model simulation of the evolution of GrIS ice slabs and aquifers (1980–2020), evaluated using radar measurements. The results show that accumulation, melt and rain rates are good predictors for the spatial distribution of ice slabs and aquifers. Both features were already present in the late 1980s, and their extent remained relatively constant until the beginning of this century, after which increased melt led to their expansion. We show that almost any transect from the coast to the ice-sheet interior will cross either an ice slab region, or an aquifer, or both.

Plain Language Summary The Greenland ice sheet is covered by a layer of old, porous snow called firn, which has the capacity to prevent surface melt runoff. The firn can however, form thick ice slabs or store large amounts of water underground. These change the fate of surface melt by respectively enhancing runoff and draining water to the ice sheet's bed. While observations have shown where these phenomena occur, it is still unknown what the exact atmospheric conditions are that lead to their formation. Here, we tackle this problem using computer simulations. Our results show that the amount of snowfall, melt and rain determine whether ice slabs or aquifers can form. The results also suggest that ice slabs and aquifers are more abundant than previously assumed, and that their observed expansion started only in the early 2000s, and they will continue to expand if the climate gets warmer and melt and rain become more abundant.

1. Introduction

Since ∼1990, increased meltwater runoff has been the dominant contributor to mass loss from the Greenland Ice Sheet (GrIS) (Enderlin et al., 2014; Mouginot et al., 2019). However, the fate of surface meltwater varies strongly in place and time (Mankoff et al., 2020). In the ablation area an efficient drainage system develops over the course of the melt season. This allows meltwater to quickly reach the edge of the ice sheet or drain to the bed via moulins and crevasses (Chu, 2014). In the accumulation zone, however, the movement of liquid water is complicated by porous, multiyear snow called firn. An estimated 45% of the total meltwater produced on the GrIS does not run off but is retained in the firn by capillary forces or refreezing (van Angelen et al., 2013). Firn thus plays an important role in moderating GrIS mass loss (Harper et al., 2012).

Ice slabs, ice layers of at least 1 m thick, have been detected inside the firn of the western and northern GrIS (Jullien et al., 2023; MacFerrin et al., 2019; Machguth et al., 2016). They limit meltwater storage and facilitate runoff (MacFerrin et al., 2019). Along the southeastern margin of the GrIS, however, high snowfall and high melt rates lead to aquifers: year-round storage of meltwater inside the firn's pore space (Forster et al., 2014; Miège et al., 2016). Liquid water remains in aquifers for years (Miller et al., 2018), draining through crevasses to the ice-sheet bed (Cicero et al., 2023; Poinar et al., 2017). This release of liquid water dampens seasonal variations of ice flow velocities (Poinar et al., 2019).

Both ice slabs and firn aquifers have expanded in the past two decades (Horlings et al., 2022; Jullien et al., 2023), but the short time series prevented a robust coupling to climatic drivers. It has been hypothesized that extreme melt events promote ice slab formation (Culberg et al., 2021; Jullien et al., 2023; Machguth et al., 2016) and that aquifer expansion is associated with decreasing cold content (Horlings et al., 2022). Here, we use observations of ice slabs and aquifers to evaluate a firn model, which enables us to study climatic drivers of GrIS ice slabs and firn aquifers over a longer period (1980–2020).

19448007, 2024, 3, Downloaded from https://agupubs.onlinelibrary.wiley.com/doi/10.1029/2023GL106613 by Utrecht University Library, M&A E-Collection, Wiley Online Library on [01/02/2024]. See the Terms and Conditions (https://onlinelibrary.wiley.com/terms-and-conditions) on Wiley Online Library for rules of use; OA articles are governed by the applicable Creative Commons License

2. Data and Methods

2.1. Model and Forcing

We use the IMAU Firn Densification Model (IMAU-FDM) version 1.2G (Brils et al., 2021). Liquid water from melt or rain can percolate into the firn layer. IMAU-FDM uses a "bucket method" for handling vertical water transport. When water passes through temperate firn, some is retained within the pores through capillary forces, called irreducible water. In IMAU-FDM, the maximum irreducible water content is 5%–15% of the layer's mass, depending on density (Coléou & Lesaffre, 1998). In a layer below the melting point, liquid water will refreeze until no more cold content or pore space is available. Any remaining liquid water is then instantaneously transported to the next layer, until either all water has refrozen or is retained as irreducible water. Here, firn and ice are treated as fully permeable (Section 4.1). Water that reaches the model's bottom is assumed to run off. The bucket method is computationally efficient but does not allow for saturated firn.

At its surface, IMAU-FDM is forced with 3-hourly mass fluxes and skin temperature from the regional climate model RACMO2.3p2, referred to as RACMO hereafter. The coupling is unidirectional, which allows for a higher vertical resolution than RACMO's internal firn model, while keeping the computational costs manageable. The GrIS surface mass balance (SMB) from RACMO has been evaluated extensively, with observations dating back to 1975 (Lenaerts et al., 2014; Noël et al., 2018; van Angelen et al., 2014). Tedstone and Machguth (2022) compared the extent of the modeled runoff area with Landsat imagery, and Smith et al. (2017) compared RACMO's runoff to in situ measurements. These studies show that RACMO is well capable of simulating the GrIS (near-)surface climate and ablation zone extent. Some caveats remain, such as compensating energy flux errors in the lower ablation zone (Noël et al., 2018), and a general overestimation of the runoff area (Tedstone & Machguth, 2022). We initialize IMAU-FDM by repeatedly running the period 1960–1980 until the firn layer is in equilibrium. The model is then run from November 1957 to January 2021 with a time step of 15 min and a spatial resolution of 5.5 km. Here, we analyze the evolution of firn after the spin-up period, from 1980 onwards.

2.2. Modeling Ice Slabs and Aquifers

A layer is considered ice if its density exceeds 830 kg m^{-3}, the approximate pore close-off density. Modeled ice layers thus have a density between 830 and 917 kg m^{-3}, consistent with field observations (Harper et al., 2012; Machguth et al., 2016; Rennermalm et al., 2022). Following MacFerrin et al. (2019) and Jullien et al. (2023), an ice layer is considered an "ice slab" if it is at least 1 m thick. Thinner layers will be referred to as "ice lenses." Given typical burial rates and ice velocities, the majority of ice slabs remain in the same model grid cell they were created in. Again following MacFerrin et al. (2019) and Jullien et al. (2023), we only consider ice in the top 20 m of firn. Grid cells with a mean negative SMB during 1960–1980 are considered ablation zone, without firn, and are excluded from the analysis. Figures S1 and S2 in Supporting Information S1 demonstrate the methodology.

We define a grid cell to contain an aquifer if, during an entire year, irreducible water is present in the firn at any depth. Irreducible water content does not allow us to say anything meaningful about the volume of stored liquid water, but this definition does allow us to map aquifer extent (Kuipers Munneke et al., 2014). Extent maps for a multi-year period represent the mean of the annual extents in this period.

2.3. Observations of Ice Slabs and Aquifers

Ice-slab observations for 2010–2018 are taken from Jullien et al. (2023), who used 550–900 MHz airborne accumulation radar from Operation Ice Bridge (OIB) (Carl et al., 2023; CReSIS, 2021). By comparing OIB to in situ measurements from ground penetrating radar, Jullien et al. (2023) obtained ice slab probabilities up to a depth of ∼20 m. These probabilities were converted into a binary ice slab extent (see Figures S2 and S3 in Supporting Information S1 for an example).

Miège et al. (2016) also used accumulation radar data to map the location of GrIS firn aquifers (2010–2014). In addition, they used the Multichannel Coherent Radar Depth Sounder (MCoRDS). Observations of bright, continuous reflectors below the surface were manually converted to a water table depth.

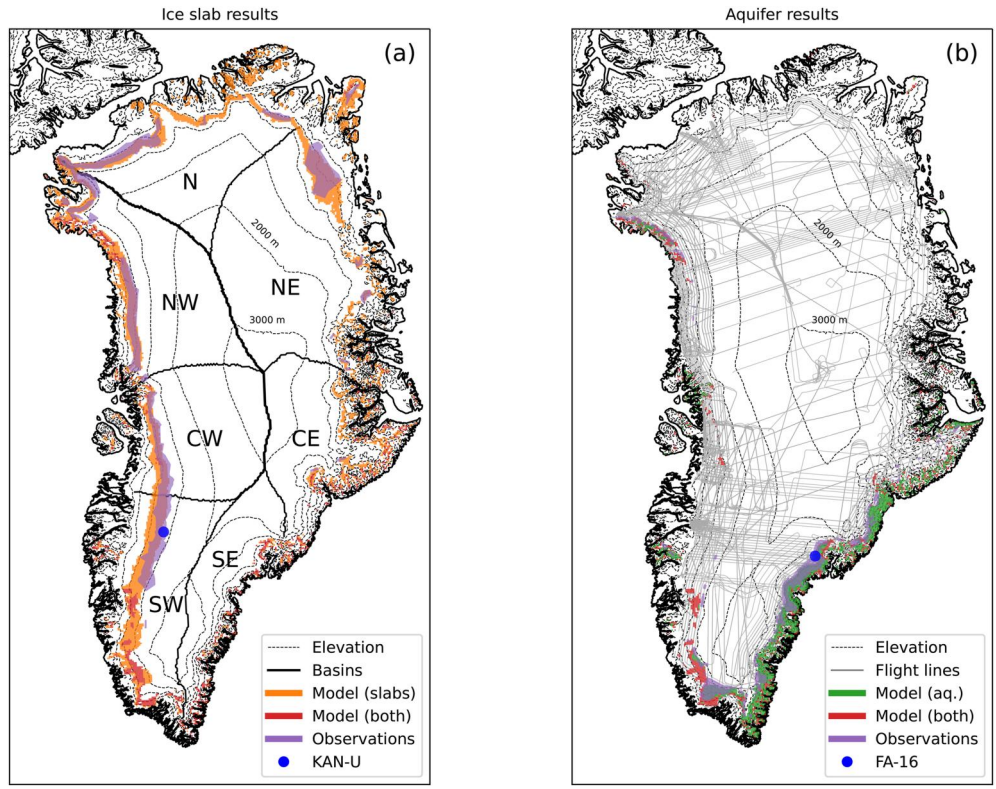

Figure 1. Locations with modeled and OIB observed (a) ice slabs for 2010–2018 (Jullien et al., 2023), and (b) aquifers during 2010–2014 (Miège et al., 2016). Full black lines in (a) represent Mouginot et al. (2019) ice sheet basins. Gray lines are OIB 2010–2018 flightlines. Blue dots represent locations of the arrows in Figure 4. Dashed gray lines indicate elevation contours at 500 m intervals.

3. Results

3.1. Spatial Distribution

Figure 1 and Figure S3 in Supporting Information S1 compare modeled (a) and observed (b) extent of ice slabs (2010–2018) and aquifers (2010–2014). IMAU-FDM simulates ice slabs in a continuous band running along most of the western and northern margin of the ice sheet's lower accumulation zone. This is in qualitative agreement with the radar observations. However, the modeled extent is more continuous, especially in the north, and extends further south. IMAU-FDM predicts 18% of the total ice slab area to occur in peripheral glaciers and ice caps, leading to a total modeled ice slab area of 230.0×10^3 km^2. This is three to four times larger than the observational estimate of the total area ($60.4–73.5 \times 10^3$ km^2), reported for the same time period (Jullien et al., 2023).

Both model and radar observations show extensive aquifers in the southeastern GrIS, where ice slabs are mostly absent. Aquifers are also modeled and observed in the northwestern GrIS and on the southern side of Maniitsoq ice cap. Unlike the observations, the model also predicts small aquifers where the CW and NW basins meet. As for ice slabs, the modeled aquifer extent is more continuous than the observations and extends to lower elevations. Modeled aquifers cover an area of 105.8×10^3 km^2, of which 17% in peripheral glaciers and ice caps. Based on OIB observations, Miège et al. (2016) derived a ~5 times smaller extent for the same period (21.9×10^3 km^2). Interestingly, IMAU-FDM also models locations containing both ice slabs and aquifers, predominantly in the far southwest and northwest, bordering regions with only aquifers and ice slabs. The total area containing both ice slabs and aquifers is 34.6×10^3 km^2.

Figure 2 and Figure S6 in Supporting Information S1 show 2010–2018 modeled "slab content" (green line) per 100 m elevation bin, defined as the total amount of ice slabs in the top 20 m of firn. Modeled slab content decreases with elevation, roughly following a logistic curve. In the south, this transition is faster and ice slabs occur

19448007, 2024, 3, Downloaded from https://agupubs.onlinelibrary.wiley.com/doi/10.1029/2023GL106613 by Utrecht University Library, M&A E-Collection, Wiley Online Library on [01/02/2024]. See the Terms and Conditions (https://onlinelibrary.wiley.com/terms-and-conditions) on Wiley Online Library for rules of use; OA articles are governed by the applicable Creative Commons License

10.1029/2023GL106613

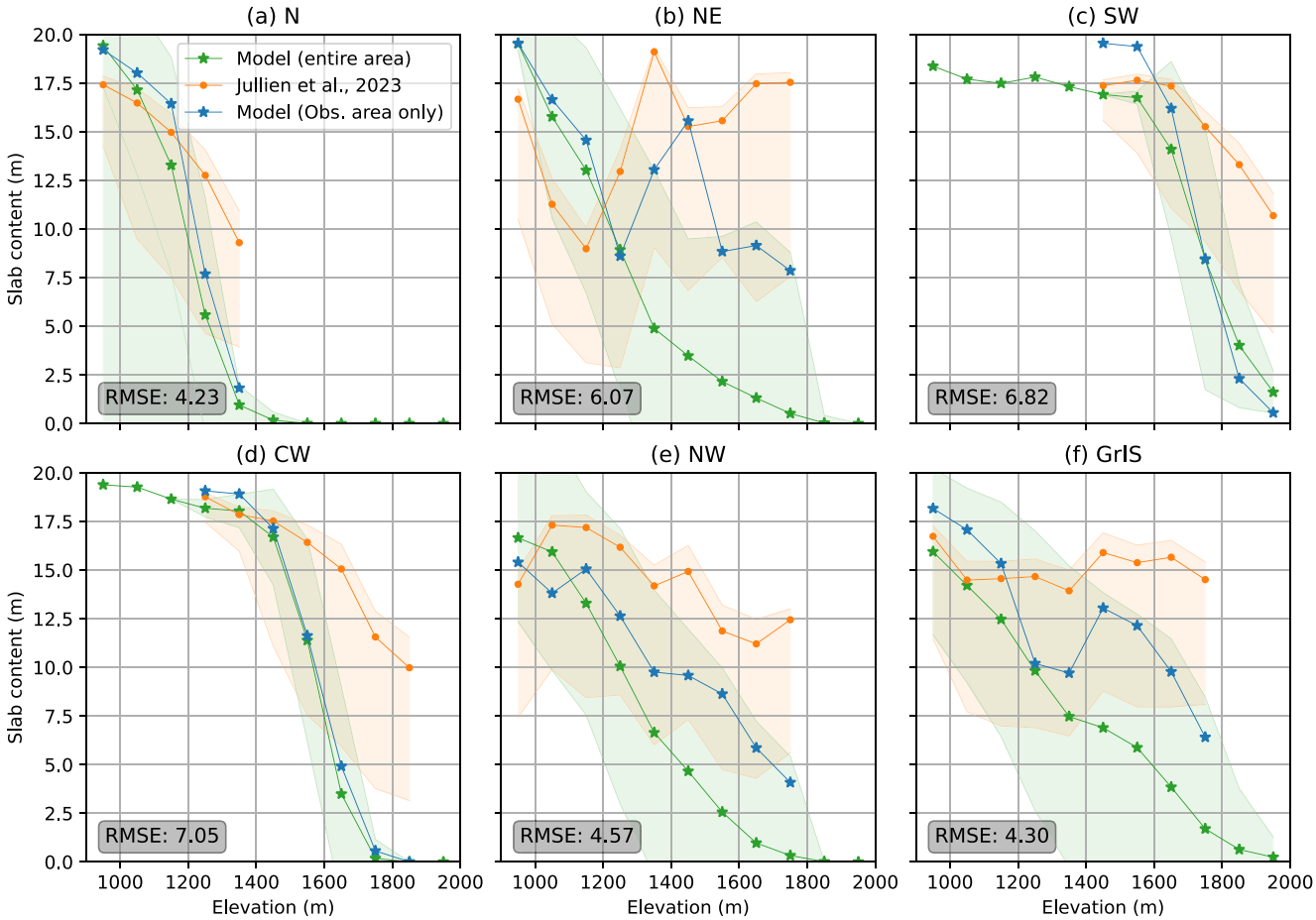

Figure 2. Modeled and observed mean ice slab content in the upper 20 m (2010–2018), in 100 m surface elevation bins for each basin (a–e) and the GrIS (f). Green lines represent averages for the entire basin, blue lines the average of model grid cells that coincide with OIB radar measurements. Shaded areas represent one standard deviation. For the orange and blue lines, only elevation bins with a large enough sample size are plotted (Figure S4 in Supporting Information S1). RMSE: root-mean squared difference between model results (blue line) and observations (orange line).

at higher elevations than in the north. When we recompute the model results using only grid cells that coincide with OIB flightlines (blue lines), there is general agreement between model and observations within the uncertainty bands. Different methods for computing the observations' standard deviation yields similar results, illustrating that the range is robust (Figure S5 in Supporting Information S1).

3.2. Temporal Evolution 1980–2020

According to the model, both ice slabs and aquifers were already widespread in the early 1980s (Figure 3). Modeled extents remained constant until the 2000s, implying that their expansion is a recent phenomenon. Ice slab extent increased stepwise. The greatest expansion was in 2012, which saw record summer melt (Nghiem et al., 2012). This is consistent with radar (Culberg et al., 2021; Jullien et al., 2023) and field observations (Machguth et al., 2016). In the following years, melt was less intense, which slowed down the expansion and even leading to a recovery in pore space in parts of southwest Greenland (Brils et al., 2023; Jullien et al., 2023; Rennermalm et al., 2022). Another, smaller jump occurred in 2015, due to large melt rates in northern Greenland (Tedesco et al., 2016). In contrast, the modeled total aquifer extent increased gradually since the early 2000s and decreased after 2012. Figure S7 and Table S1 in Supporting Information S1 show that recent changes in ice slabs in SW and aquifers in SE agree broadly with observed changes (Horlings et al., 2022; Jullien et al., 2023).

19448007, 2024, 3, Downloaded from https://agupubs.onlinelibrary.wiley.com/doi/10.1029/2023GL106613 by Utrecht University Library, M&A E-Collection, Wiley Online Library on [01/02/2024]. See the Terms and Conditions (https://onlinelibrary.wiley.com/terms-and-conditions) on Wiley Online Library for rules of use; OA articles are governed by the applicable Creative Commons License

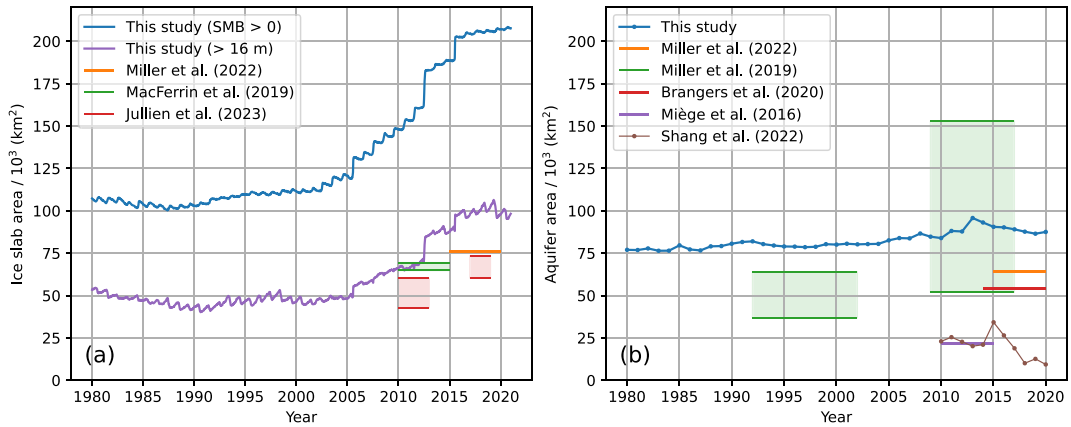

Figure 3. Time series of modeled total extent of ice slabs (a) and aquifers (b) on the contiguous GrIS, and observational estimates. Panel (a) shows model results for two different ablation zone thresholds, SMB = 0 (blue) or 16 m slab content (purple). Horizontal lines and shaded areas indicate observational estimates of total ice slab and aquifer extent and their uncertainties (Brangers et al., 2020; Jullien et al., 2023; MacFerrin et al., 2019; Miège et al., 2016; Miller et al., 2020, 2022; Shang et al., 2022).

3.3. Climatic Drivers

Figure 4 shows that the presence of aquifers, ice slabs and ice lenses is strongly governed by the rates of accumulation and surface liquid water input (melt plus rain). With 1960–1980 averages, we approximate an equilibrium situation, since this period is also used as the model's reference (spin-up) period. Each type of firn facies occupies a distinct area in Figure 4, with little overlap. In a climate with little melt and rain, a firn layer forms without ice slabs or aquifers (purple), whereas if melt strongly exceeds accumulation, no firn can exist (red). Dashed lines indicate the theoretical boundaries between ablation/accumulation zones and the ice slab/no ice slab zones (Text S1 in Supporting Information S1). For low-accumulation sites, a sufficiently high melt rate leads to ice lenses. Higher melt rates lead to the formation of ice slabs. At higher accumulation rates, insulation of the liquid water from the cold atmosphere limits refreezing, and aquifers form instead. Interestingly, in a narrow band where melt roughly equals accumulation, aquifers and ice slabs are predicted to occur simultaneously. At higher melt rates, aquifers eventually disappear as the system transitions toward the ice-slab-only regime. Our

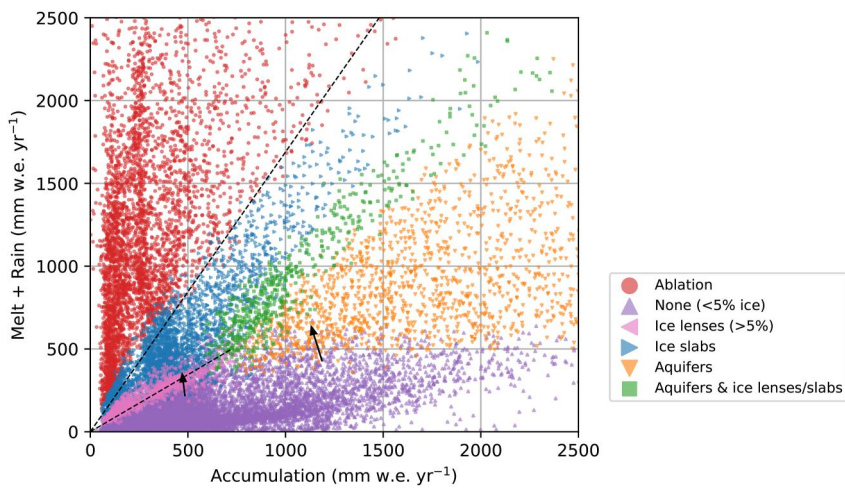

Figure 4. Average 1960–1980 combined melt and rain rates as a function of accumulation rate for all IMAU-FDM grid cells. Symbols indicate presence of ice lenses/slabs or aquifers for at least half of the 1960–1980 period. Arrows connect 1960–1980 (arrow base) with 2000–2020 (head) averages for two selected locations (Figure 1a): KAN-U (left) and FA-16 (right). Dashed lines represent melt/rain over accumulation (MoA) ratios of ~0.7 and ~1.7 (Text S1 in Supporting Information S1).

19448007, 2024, 3, Downloaded from https://agupubs.onlinelibrary.wiley.com/doi/10.1029/2023GL106613 by Utrecht University Library, M&A E-Collection, Wiley Online Library on [01/02/2024]. See the Terms and Conditions (https://onlinelibrary.wiley.com/terms-and-conditions) on Wiley Online Library for rules of use; OA articles are governed by the applicable Creative Commons License

19448007, 2024, 3, Downloaded from https://agupubs.onlinelibrary.wiley.com/doi/10.1029/2023GL106613 by Utrecht University Library, M&A E-Collection, Wiley Online Library on [01/02/2024]. See the Terms and Conditions (https://onlinelibrary.wiley.com/terms-and-conditions) on Wiley Online Library for rules of use; OA articles are governed by the applicable Creative Commons License

study confirms that at least ~500 mm w.e. y^{-1} of surface melt is required to form aquifers (Kuipers Munneke et al., 2014). Then, liquid water reaches greater depths that prevent it from refreezing in winter. The aquifer results are also consistent with Forster et al. (2014). Figures 1 and 4 also imply that any transect from the coast to the ice-sheet interior will cross either an ice slab region, or an aquifer, or both. The only exceptions are in the NE and SE, where model resolution might be too coarse to resolve the steep topography.

4. Discussion

4.1. Evaluation of the Model Results

4.1.1. Ice Slabs

Comparing observed and modeled ice slabs and aquifers is not straightforward. The model reproduces the OIB results qualitatively, but there are some notable differences. Most striking is the larger total modeled extent. Table S2 in Supporting Information S1 shows that 86% of observed ice slab locations agree with the model. This suggests that low OIB coverage explains an important part of the difference. For instance, an important contribution to the difference comes from peripheral glaciers and ice caps, where OIB has low coverage. Similarly, the SW, CE, and NE ice sheet basins contain areas with lower coverage. Another uncertainty is the ice-slab-ablation-area boundary. Here, this boundary is set to the modeled 1960–1980 equilibrium line (SMB = 0). In reality, however, the transition from the ice slab area to the ablation zone is neither steady nor sharp (Figure 2 and Figure S10 in Supporting Information S1). MacFerrin et al. (2019) and Jullien et al. (2023) excluded parts of flightlines that contain more than 16 m of ice, assuming those are situated in the ablation zone. If we use the same threshold for the model results, this significantly decreases the difference, but erroneously decreases the width of the ice slab zone (purple line in Figure 3a and Figure S8 in Supporting Information S1). The radar also has trouble detecting ice slabs in the first ~1.5 m of firn, owing to additional uncertainty near the surface (Text S2 in Supporting Information S1).

Despite the larger extent, the modeled slab content is lower at high elevations while the transition to a higher slab content is more abrupt (Figure 2). There are two reasons for this. Firstly, at higher elevations OIB flightlines are biassed toward locations with a lower SMB (Figure S9 in Supporting Information S1). Recalculating the modeled slab content while excluding the areas not sampled by OIB significantly improves the agreement, often falling within one standard deviation (blue lines in Figure 2). Secondly, ice is treated as permeable in IMAU-FDM whereas Jullien et al. (2023) observed that ice slabs grow mostly by accretion on top. Therefore, at low melt rates, the formation of multiple thinner ice lenses is more likely in the model. When these layers merge, they are classified as slabs and the content increases sharply. Extreme melt years, however, can produce modeled ice slabs within a single summer, even at higher elevations. As a result, extreme melt years determine the total ice slab extent, rather than successive moderate melt years, and the total extent is not impacted much by treating ice as permeable.

4.1.2. Firn Aquifers

Just as for ice slabs, the aquifer extent from OIB likely poses a lower limit. Of the observed aquifers, 62% is also modeled (Table S3 in Supporting Information S1). It is possible that the presence of ice layers above the water table reduces the backscatter, preventing their observation (Forster et al., 2014). Radar also requires enough water to be present for the detection of an aquifer, whereas the model aquifer definition considers any amount of water, at all depths. The bucket method in IMAU-FDM only allows irreducible liquid water in firn, whereas an actual aquifer often contains fully saturated firn. This possibly leads to a too large temporal variability in aquifer extent, in response to variability in the atmospheric forcing. However, this is not what we find. For example, after 2012 the melt in the SE decreased (Brils et al., 2023), leading to a smaller aquifer extent. This decline agrees with observations before and after 2012 (Horlings et al., 2022; Shang et al., 2022). Lateral flow of water is not included in IMAU-FDM either, whereas it has been observed within aquifers (Miller et al., 2018). However, the measured specific discharge is negligibly low (1.4×10^2 m yr^{-1}). Firn aquifers are known to drain in heavily crevassed areas (Cicero et al., 2023; Poinar et al., 2017), a process that is not included in the firn model. This could explain why modeled aquifers extend to lower elevations (Figure 1 and Figure S7 in Supporting Information S1). The width of the ablation zone in the SE basin is in the same range as IMAU-FDM's grid size, potentially leading to a poor representation of the ablation zone extent.

19448007, 2024, 3, Downloaded from https://agupubs.onlinelibrary.wiley.com/doi/10.1029/2023GL106613 by Utrecht University Library, M&A E-Collection, Wiley Online Library on [01/02/2024]. See the Terms and Conditions (https://onlinelibrary.wiley.com/terms-and-conditions) on Wiley Online Library for rules of use; OA articles are governed by the applicable Creative Commons License

4.1.3. Simultaneous Occurrence of Ice Slabs and Aquifers

The red areas in Figure 1a represent combined ice slab/aquifer locations in the model. While OIB did not detect ice slabs in the southwestern tip of the ice sheet, Miller et al. (2022) reported ice slabs located next to aquifers in this region. Their algorithm, however, does not allow ice slabs and aquifers to exist at the same location. And although on a coarser resolution, the firn models SNOWPACK and CFM-CSFC also simulate ice in the upper 20 m of firn in the southern GrIS (Thompson-Munson et al., 2023). These results are in line with our prediction of a mixture of ice slabs and aquifers in this region. Results from Miège et al. (2016) and Culberg et al. (2021) suggest that aquifers can be perched above ice slabs, and thin ice lenses have been observed directly above them (Forster et al., 2014). Liquid water has a bright reflection at the aquifer surface, making it impossible to detect ice slabs beneath aquifers. For this reason, MacFerrin et al. (2019) and Jullien et al. (2023) manually excluded regions that contain surface lakes or visible subsurface aquifers. This excludes the simultaneous observation of ice slabs and aquifers with accumulation radar. Finally, we note that locations where ice slabs and aquifers co-exist coincide with regions with high rainfall (Huai et al., 2022). Rainfall coincides with warm and cloudy conditions, which suppress refreezing (Bennartz et al., 2013; Van Tricht et al., 2016). Thus, rainfall might favor aquifer formation whereas melt favors ice slab formation.

4.2. Implications in a Warming Climate

Figure 4 suggests that in a warmer climate, an increase in melt will lead to expansion of both ice slab and aquifer regions. The arrows in Figure 4a connect the 1960–1980 and 2000–2020 mean climates at two locations, KAN-U and FA-16 (Figure 1), illustrating how firn can change over time. Observations over the last decade show that the firn at KAN-U now contains a lot of ice layers (MacFerrin et al., 2019; Rennermalm et al., 2022) and that FA-16 presently contains an aquifer (Miller et al., 2018). Figure 3 suggests that the ice slab expansion started in the mid 2000s and accelerated over time. This acceleration is partly due to the nonlinear increase of melt with temperature (Trusel et al., 2018), but also because the topography of the ice sheet flattens at higher elevations, leading to larger areas experiencing an increase in melt (Machguth et al., 2016; van As et al., 2017).

Regions containing ice slabs enhance surface runoff and facilitate the formation of supraglacial streams (Tedstone & Machguth, 2022). This enhances the melt-albedo feedback. On the other hand, regions with aquifers are mostly devoid of such supraglacial features and store melt within the aquifer. This storage is temporary, and most of the water will drain to the bed through crevasses (Miller et al., 2018). Ice slabs and aquifers thus have an opposite effect on the hydrology: while ice slabs enhance surface runoff, aquifers delay it, and while aquifers release water to the bed, ice slabs locally prevent this. Figure 4 suggests that when melt increases, aquifer locations can turn into a location with ice slabs, leading to a fundamental change in ice-sheet hydrology. This transition could occur more frequently in a warmer climate.

5. Conclusions

In this paper, we use the firn model IMAU-FDM, forced with the regional climate model RACMO, to identify climatic drivers of ice slabs and aquifers on the GrIS and their contemporary area changes. Compared to observations, the model performs qualitatively well, but simulates larger and more continuous ice slabs (233.0×10^3 km^2) and aquifers (105.0×10^3 km^2), of which many occur outside of the contiguous ice sheet. Their total modeled area remained relatively constant between 1980 and the early 2000s, after which they expanded inland. According to the model, any transect from the coast to the ice-sheet interior will cross either an ice slab region, or an aquifer, or both. We show that available liquid water (melt and rain) and accumulation are good predictors for the occurrence of ice slabs and aquifers. Our results also suggest that, in a warming climate, increasing melt and rain can turn an aquifer region, which delays runoff, into an ice slab region, which facilitates runoff, representing a potentially fundamental change in the ice sheet's hydrology.

Data Availability Statement

The model output used in this paper can be found on Zenodo (https://doi.org/10.5281/zenodo.8386406 or https://zenodo.org/records/8386406). OIB data on aquifers (Miège et al., 2016) and ice slabs (Jullien et al., 2023) can be found with their DOIs https://doi.org/10.18739/A2985M (https://arcticdata.io/catalog/view/doi:10.18739/A2985M) and https://doi.org/10.5281/zenodo.7505426 (https://zenodo.org/records/7505426), respectively. The

firn-aquifer extents from Horlings et al. (2022) are available through the NSF Arctic Data Center at: https://arcticdata.io/catalog/view/doi:10.18739/A2JM23H40.

Acknowledgments
MB, PKM and MvdB acknowledge funding from the Netherlands Earth System Science Centre (NESSC), financed by the Ministry of Education, Culture and Science (OCW Grant 024.002.001). This publication was also supported by PROTECT. This project has received funding from the European Union's Horizon 2020 research and innovation programme under Grant agreement No 869304, PROTECT contribution number 86. NJ, AT and HM are funded by the European Research Council (ERC) under the European Union's Horizon 2020 research and innovation programme (project acronym CASSANDRA, grant agreement No. 818994). We acknowledge ECMWF for computational time on their supercomputers. We thank Kristin Poinar and an anonymous reviewer for very helpful comments.

References

Bennartz, R., Shupe, M. D., Turner, D. D., Walden, V. P., Steffen, K., Cox, C. J., et al. (2013). July 2012 Greenland melt extent enhanced by low-level liquid clouds. *Nature*, *496*(7443), 83–86. https://doi.org/10.1038/nature12002

Brangers, I., Lievens, H., Miège, C., Demuzere, M., Brucker, L., & De Lannoy, G. J. M. (2020). Sentinel-1 detects firn aquifers in the Greenland ice sheet. *Geophysical Research Letters*, *47*(3). https://doi.org/10.1029/2019GL085192

Brils, M., Kuipers Munneke, P., Berg, W. J. V. D., & Broeke, M. V. D. (2021). Improved representation of the contemporary Greenland ice sheet firn layer by IMAU-FDM v1. 2G. *Geoscientific Model Development*, *15*, 1–28. https://doi.org/10.5194/gmd-15-7121-2022

Brils, M., Kuipers Munneke, P., & van den Broeke, M. R. (2023). Spatial response of Greenland's firn layer to NAO variability. *Journal of Geophysical Research: Earth Surface*, *128*(8), e2023JF007082. https://doi.org/10.1029/2023JF007082

Carl, L., Lewis, C., Gogineni, S. P., Rodriguez, F., Paden, J., & Li, J. (2023). IceBridge accumulation radar L1B geolocated radar echo strength profiles, 2010, 2011, 2012, 2013, 2014, 2017, 2018 [Dataset]. National Snow and Ice Data Center. Digital media. Retrieved from https://data.cresis.ku.edu/data/accum/

Chu, V. W. (2014). Greenland ice sheet hydrology: A review. *Progress in Physical Geography*, *38*(1), 19–54. https://doi.org/10.1177/0309133313507075

Cicero, E., Poinar, K., Jones-Ivey, R., Petty, A. A., Sperhac, J. M., Patra, A., & Briner, J. P. (2023). Firn aquifer water discharges into crevasses across Southeast Greenland. *Journal of Glaciology*, *69*(277), 1–14. https://doi.org/10.1017/jog.2023.25

Coléou, C., & Lesaffre, B. (1998). Irreducible water saturation in snow: Experimental results in a cold laboratory. *Annals of Glaciology*, *26*(2), 64–68. https://doi.org/10.3189/1998aog26-1-64-68

CReSIS. (2021). Accumulation radar data, 2002, 2003, 2010, 2011, 2012, 2013, 2014, 2017, 2018 [Dataset]. Digital Media. Retrieved from https://data.cresis.ku.edu/data/accum/

Culberg, R., Schroeder, D. M., & Chu, W. (2021). Extreme melt season ice layers reduce firn permeability across Greenland. *Nature Communications*, *12*(1), 1–9. https://doi.org/10.1038/s41467-021-22656-5

Enderlin, E. M., Howat, I. M., Jeong, S., Noh, M.-J., van Angelen, J. H., & van den Broeke, M. R. (2014). An improved mass budget for the Greenland ice sheet. *Geophysical Research Letters*, *41*(3), 866–872. https://doi.org/10.1002/2013GL059010

Forster, R. R., Box, J. E., van den Broeke, M. R., Miège, C., Burgess, E. W., van Angelen, J. H., et al. (2014). Extensive liquid meltwater storage in firn within the Greenland ice sheet. *Nature Geoscience*, *7*(2), 95–98. https://doi.org/10.1038/ngeo2043

Harper, J., Humphrey, N., Pfeffer, W. T., Brown, J., & Fettweis, X. (2012). Greenland ice-sheet contribution to sea-level rise buffered by meltwater storage in firn. *Nature*, *491*(7423), 240–243. https://doi.org/10.1038/nature11566

Horlings, A. N., Christianson, K., & Miège, C. (2022). Expansion of firn aquifers in southeast Greenland. *Journal of Geophysical Research: Earth Surface*, *127*(10), e2022JF006753. https://doi.org/10.1029/2022JF006753

Huai, B., van den Broeke, M. R., Reijmer, C. H., & Noël, B. (2022). A daily 1-km resolution Greenland rainfall climatology (1958–2020) from statistical downscaling of a regional atmospheric climate model. *Journal of Geophysical Research: Atmospheres*, *127*(17), e2022JD036688. https://doi.org/10.1029/2022JD036688

Jullien, N., Tedstone, A. J., Machguth, H., Karlsson, N. B., & Helm, V. (2023). Greenland ice sheet ice slab expansion and thickening. *Geophysical Research Letters*, *50*(10), e2022GL100911. https://doi.org/10.1029/2022GL100911

Kuipers Munneke, P., Ligtenberg, S. R. M., Van den Broeke, M. R., Van Angelen, J. H., & Forster, R. R. (2014). Explaining the presence of perennial liquid water bodies in the firn of the Greenland Ice Sheet. *Geophysical Research Letters*, *41*(2), 476–483. https://doi.org/10.1002/2013GL058389

Lenaerts, J. T. M., Smeets, C. J. P. P., Nishimura, K., Eijkelboom, M., Boot, W., Van den Broeke, M. R., & Van de Berg, W. J. (2014). Drifting snow measurements on the Greenland Ice Sheet and their application for model evaluation. *The Cryosphere*, *8*(2), 801–814. https://doi.org/10.5194/tc-8-801-2014

MacFerrin, M., Machguth, H., van As, D., Charalampidis, C., Stevens, C. M., Heilig, A., et al. (2019). Rapid expansion of Greenland's low-permeability ice slabs. *Nature*, *573*(7774), 403–407. https://doi.org/10.1038/s41586-019-1550-3

Machguth, H., Macferrin, M., van As, D., Box, J. E., Charalampidis, C., Colgan, W., et al. (2016). Greenland meltwater storage in firn limited by near-surface ice formation. *Nature Climate Change*, *6*(4), 390–393. https://doi.org/10.1038/nclimate2899

Mankoff, K. D., Noël, B., Fettweis, X., Ahlstrøm, A. P., Colgan, W., Kondo, K., et al. (2020). Greenland liquid water discharge from 1958 through 2019. *Earth System Science Data*, *12*(4), 2811–2841. https://doi.org/10.5194/essd-12-2811-2020

Miège, C., Forster, R. R., Brucker, L., Koenig, L. S., Solomon, D. K., Paden, J. D., et al. (2016). Spatial extent and temporal variability of Greenland firn aquifers detected by ground and airborne radars. *Journal of Geophysical Research: Earth Surface*, *121*(12), 2381–2398. https://doi.org/10.1002/2016JF003869

Miller, J. Z., Culberg, R., Long, D. G., Shuman, C. A., Schroeder, D. M., & Brodzik, M. J. (2022). An empirical algorithm to map perennial firn aquifers and ice slabs within the Greenland Ice Sheet using satellite L-band microwave radiometry. *The Cryosphere*, *16*(1), 103–125. https://doi.org/10.5194/tc-16-103-2022

Miller, J. Z., Long, D. G., Jezek, K. C., Johnson, J. T., Brodzik, M. J., Shuman, C. A., et al. (2020). Brief communication: Mapping Greenland's perennial firn aquifers using enhanced-resolution L-band brightness temperature image time series. *The Cryosphere*, *14*(9), 2809–2817. https://doi.org/10.5194/tc-14-2809-2020

Miller, O., Solomon, D. K., Miège, C., Koenig, L., Forster, R., Schmerr, N., et al. (2018). Direct evidence of meltwater flow within a firn aquifer in southeast Greenland. *Geophysical Research Letters*, *45*(1), 207–215. https://doi.org/10.1002/2017GL075707

Mouginot, J., Rignot, E., Bjørk, A. A., van den Broeke, M., Millan, R., Morlighem, M., et al. (2019). Forty-six years of Greenland Ice Sheet mass balance from 1972 to 2018. *Proceedings of the National Academy of Sciences of the United States of America*, *116*(19), 9239–9244. https://doi.org/10.1073/pnas.1904242116

Nghiem, S. V., Hall, D. K., Mote, T. L., Tedesco, M., Albert, M. R., Keegan, K., et al. (2012). The extreme melt across the Greenland ice sheet in 2012. *Geophysical Research Letters*, *39*(20), 6–11. https://doi.org/10.1029/2012GL053611

Noël, B., van de Berg, W. J., van Wessem, J. M., van Meijgaard, E., van As, D., Lenaerts, J. T. M., et al. (2018). Modelling the climate and surface mass balance of polar ice sheets using RACMO2 – Part 1: Greenland (1958–2016). *The Cryosphere*, *12*(3), 811–831. https://doi.org/10.5194/tc-12-811-2018

19448007, 2024, 3, Downloaded from https://agupubs.onlinelibrary.wiley.com/doi/10.1029/2023GL106613 by Utrecht University Library, M&A E-Collection, Wiley Online Library on [01/02/2024]. See the Terms and Conditions (https://onlinelibrary.wiley.com/terms-and-conditions) on Wiley Online Library for rules of use; OA articles are governed by the applicable Creative Commons License

Poinar, K., Dow, C. F., & Andrews, L. C. (2019). Long-term support of an active subglacial hydrologic system in southeast Greenland by firn aquifers. *Geophysical Research Letters*, *46*(9), 4772–4781. https://doi.org/10.1029/2019GL082786

Poinar, K., Joughin, I., Lilien, D., Brucker, L., Kehrl, L., & Nowicki, S. (2017). Drainage of southeast Greenland firn aquifer water through crevasses to the bed. *Frontiers in Earth Science*, *5*, 1–15. https://doi.org/10.3389/feart.2017.00005

Rennermalm, Å. K., Hock, R., Covi, F., Xiao, J., Corti, G., Kingslake, J., et al. (2022). Shallow firn cores 1989-2019 in southwest Greenland's percolation zone reveal decreasing density and ice layer thickness after 2012. *Journal of Glaciology*, *68*(269), 431–442. https://doi.org/10.1017/jog.2021.102

Shang, X., Cheng, X., Zheng, L., Liang, Q., & Chi, Z. (2022). Decadal changes in Greenland ice sheet firn aquifers from radar scatterometer. *Remote Sensing*, *14*(9), 1–19. https://doi.org/10.3390/rs14092134

Smith, L. C., Yang, K., Pitcher, L. H., Overstreet, B. T., Chu, V. W., Rennermalm, Å. K., et al. (2017). Direct measurements of meltwater runoff on the Greenland ice sheet surface. *Proceedings of the National Academy of Sciences of the United States of America*, *114*(50), E10622–E10631. https://doi.org/10.1073/pnas.1707743114

Tedesco, M., Mote, T., Fettweis, X., Hanna, E., Jeyaratnam, J., Booth, J. F., et al. (2016). Arctic cut-off high drives the poleward shift of a new Greenland melting record. *Nature Communications*, *7*(1), 11723. https://doi.org/10.1038/ncomms11723

Tedstone, A. J., & Machguth, H. (2022). Increasing surface runoff from Greenland's firn areas. *Nature Climate Change*, *12*(7), 672–676. https://doi.org/10.1038/s41558-022-01371-z

Thompson-Munson, M., Wever, N., Stevens, C. M., Lenaerts, J. T. M., & Medley, B. (2023). An evaluation of a physics-based firn model and a semi-empirical firn model across the Greenland Ice Sheet (1980–2020). *The Cryosphere*, *17*(5), 2185–2209. https://doi.org/10.5194/tc-17-2185-2023

Trusel, L. D., Das, S. B., Osman, M. B., Evans, M. J., Smith, B. E., Fettweis, X., et al. (2018). Nonlinear rise in Greenland runoff in response to post-industrial Arctic warming. *Nature*, *564*(7734), 104–108. https://doi.org/10.1038/s41586-018-0752-4

van Angelen, J. H., Lenaerts, T. T. M., van den Broeke, M. R., Fettweis, X., & van Meijgaard, E. (2013). Rapid loss of firn pore space accelerates 21st century Greenland mass loss. *Geophysical Research Letters*, *40*(10), 2109–2113. https://doi.org/10.1002/grl.50490

van Angelen, J. H., Van den Broeke, M. R., Wouters, B., & Lenaerts, J. T. M. (2014). Contemporary (1960–2012) evolution of the climate and surface mass balance of the Greenland ice sheet. *Surveys in Geophysics*, *35*(5), 1155–1174. https://doi.org/10.1007/s10712-013-9261-z

van As, D., Bech Mikkelsen, A., Holtegaard Nielsen, M., Box, J. E., Claesson Liljedahl, L., Lindbäck, K., et al. (2017). Hypsometric amplification and routing moderation of Greenland ice sheet meltwater release. *The Cryosphere*, *11*(3), 1371–1386. https://doi.org/10.5194/tc-11-1371-2017

Van Tricht, K., Lhermitte, S., Lenaerts, J. T. M., Gorodetskaya, I. V., L'Ecuyer, T. S., Noël, B., et al. (2016). Clouds enhance Greenland ice sheet meltwater runoff. *Nature Communications*, *7*(1), 10266. https://doi.org/10.1038/ncomms10266

References From the Supporting Information

Clerx, N., Machguth, H., Tedstone, A., Jullien, N., Wever, N., Weingartner, R., & Roessler, O. (2022). In situ measurements of meltwater flow through snow and firn in the accumulation zone of the SW Greenland Ice Sheet. *The Cryosphere*, *16*(10), 4379–4401. https://doi.org/10.5194/tc-16-4379-2022

Pfeffer, W. T., Meier, M. F., & Illangasekare, T. H. (1991). Retention of Greenland runoff by refreezing: Implications for projected future sea level change. *Journal of Geophysical Research*, *96*(C12), 22117–22124. https://doi.org/10.1029/91jc02502

19448007, 2024, 3, Downloaded from https://agupubs.onlinelibrary.wiley.com/doi/10.1029/2023GL106613 by Utrecht University Library, M&A E-Collection, Wiley Online Library on [01/02/2024]. See the Terms and Conditions (https://onlinelibrary.wiley.com/terms-and-conditions) on Wiley Online Library for rules of use; OA articles are governed by the applicable Creative Commons License